Quantitative MRI in hypomyelinating disorders

Correlation with motor handicap

Marjan E. Steenweg, MD, PhD
Nicole I. Wolf, MD, PhD
Wessel N. van Wieringen, PhD
Frederik Barkhof, MD, PhD
Marjo S. van der Knaap, MD, PhD*
Petra J.W. Pouwels, PhD*

Correspondence to Dr. Pouwels: pjw.pouwels@vumc.nl

ABSTRACT

Objective: To assess the correlation of tissue parameters estimated by quantitative magnetic resonance (MR) techniques and motor handicap in patients with hypomyelination.

Methods: Twenty-eight patients with different causes of hypomyelination (12 males, 16 females; mean age 10 years) and 61 controls (33 males, 28 females; mean age 8 years) were prospectively investigated. We quantified T2 relaxation time, magnetization transfer ratio, fractional anisotropy, mean, axial, and radial diffusivities, and brain metabolites. We performed measurements in the splenium, parietal deep white matter, and corticospinal tracts in the centrum semiovale. We further analyzed diffusion measures using tract-based spatial statistics. We estimated severity of motor handicap by the gross motor function classification system. We evaluated correlation of handicap with MR measures by linear regression analyses.

Results: Fractional anisotropy, magnetization transfer ratio, choline, and *N*-acetylaspartate/creatine ratio were lower and diffusivities, T2 values, and inositol were higher in patients than in controls. Tract-based spatial statistics showed that these changes were widespread for fractional anisotropy (96% of the white matter skeleton), radial (93%) and mean (84%) diffusivity, and less so for axial diffusivity (20%). Correlation with handicap yielded radial diffusivity and *N*-acetylaspartate/creatine ratio as strongest independent explanatory variables.

Conclusions: Gross motor function classification system grades are in part explained by MR measures. They indicate that mainly lack of myelin and, to a lesser degree, loss of axonal integrity codetermine the degree of motor handicap in patients with hypomyelinating disorders. These MR measures can be used to evaluate strategies that are aimed at promotion of myelination.
Neurology® 2016;87:752–758

GLOSSARY

AD = axial diffusivity; **CSI** = chemical shift imaging; **DTI** = diffusion tensor imaging; **FA** = fractional anisotropy; **GMFCS** = gross motor function classification system; **MD** = mean diffusivity; **MR** = magnetic resonance; **MTR** = magnetization transfer ratio; **NAA** = *N*-acetylaspartylglutamate; **RD** = radial diffusivity; **ROI** = region of interest; **TBSS** = tract-based spatial statistics; **TE** = echo time; **TFCE** = threshold-free cluster enhancement; **TR** = repetition time; **WM** = white matter.

Quantitative magnetic resonance (MR) techniques provide information on histopathology of brain white matter (WM) disorders.[1–9] In this study, we focused on hypomyelinating disorders, defined by permanent lack of myelin deposited. Hypomyelination can be diagnosed by MRI based on a pattern of mildly hyperintense T2 signal (figure 1A) and mildly hypo-, iso-, or hyperintense T1 signal of the WM relative to the cortex (figure 1B), depending on myelin content.[10] Follow-up MRI at least 6 months later and at an age older than 1 or preferably 2 years should show no myelination progress.[10]

Clinically, hypomyelination is associated with variable handicap ranging from walking without support and attending regular school to wheelchair dependency and absence of speech.[11] The variation in handicap is unexplained; conventional MRI does not show clear differences in myelin content. These observations bring into question the relative importance of myelin,

Editorial, page 748

Supplemental data at Neurology.org

*These authors contributed equally to this work as senior authors.

From the Department of Child Neurology (M.E.S., N.I.W., M.S.v.d.K.), VU University Medical Center, and Neuroscience Campus Amsterdam; Department of Clinical Epidemiology and Biostatistics (W.N.v.W.), VU University Medical Center; Department of Mathematics (W.N.v.W.), and Department of Functional Genomics, Center for Neurogenomics and Cognitive Research (M.S.v.d.K., P.J.W.P.), VU University, Amsterdam; and Departments of Radiology (F.B.) and Physics and Medical Technology (P.J.W.P.), VU University Medical Center, Amsterdam, the Netherlands.

Go to Neurology.org for full disclosures. Funding information and disclosures deemed relevant by the authors, if any, are provided at the end of the article.

Figure 1 Examples of FA, RD, MTR map, T2 map, and CSI spectrum

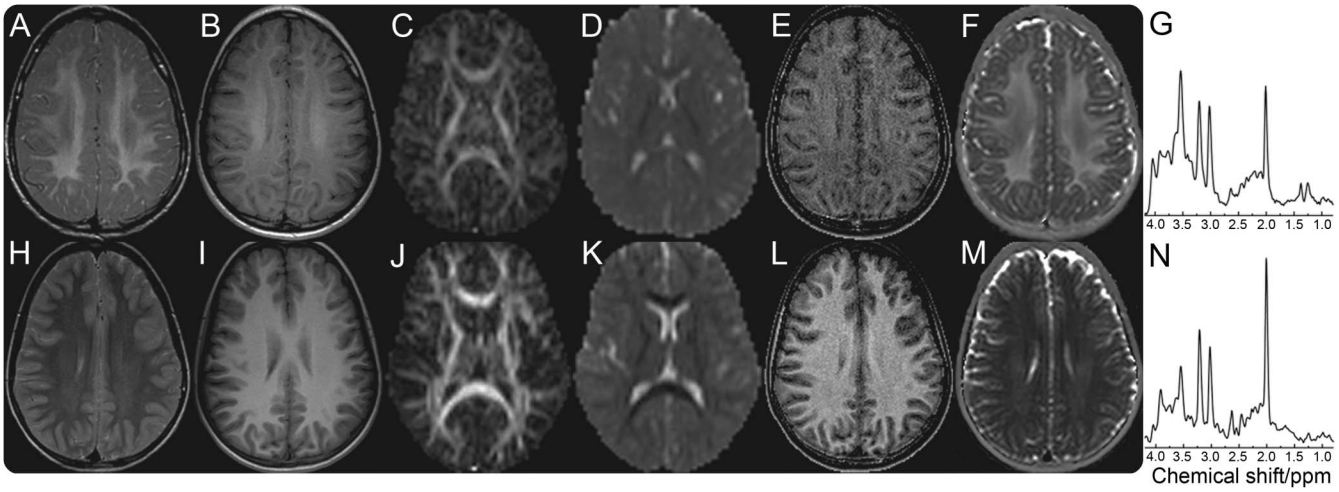

Male patient, age 7 years, with Pelizaeus-Merzbacher disease: T2-weighted (A) and T1-weighted (B) MRIs, FA map (C), and RD map (D) at the level of the centrum semiovale, MTR map (E) and T2 map (F) at the level of the CSI slice and CSI spectrum of one voxel in the parietal white matter (G). Matching images of a control, age 8 years, are shown (H–N). Corresponding maps (in the same column) have identical center-window levels for visual comparison. On the T2-weighted image of the patient, the signal of the corona radiata is less hyperintense than the surrounding white matter, suggesting more myelin deposition. This was not the case for all patients. CSI = chemical shift imaging; FA = fractional anisotropy; MTR = magnetization transfer ratio; RD = radial diffusivity.

especially compared to axonal integrity. Such questions are fundamental when considering therapies that are aimed at promotion of myelination.[12]

Previous studies of quantitative MR in hypomyelination showed that hypomyelinating disorders are generally characterized by results that are close to normal.[6,8] In the present study, we aimed to assess the correlation of tissue measures as estimated by quantitative MR techniques and degree of motor handicap in patients with hypomyelination with the hypothesis that the myelin content, estimated by quantitative MRI measures, codetermines the severity of handicap. We included axial diffusivity (AD) and radial diffusivity (RD) because AD was found to correlate with axonal integrity[13,14] and RD with intactness of myelin.[15,16]

METHODS

Standard protocol approvals, registrations, and patient consents. This prospective case-control study was performed with approval of the institutional review board and consent of patients and/or parents.

Participants. Between January 2007 and June 2011, 28 patients (table 1) underwent MRI, who fulfilled the following inclusion criteria: (1) DNA-proven hypomyelinating disorder, or (2) stable substantial deficit in myelination on 2 consecutive MRIs with an interval of at least 6 months and the second MRI in the second year or later, or (3) severe deficit in myelination on MRI in a child older than 2 years, making it unlikely that normal myelination will ever be achieved.[10] Four of these 28 patients had 2 quantitative MRIs during this period. The best quality and most complete MRI was used for analysis; if the quality was equal, the first was chosen. Using this strategy, the first MRI was analyzed in 2 cases and the second in the other two. Experienced investigators (N.I.W., M.S.v.d.K.) visually rated the MRI scans. Twelve patients were male, 16 were female; age range was 0.5 to 47 years (mean age ± SD: 11.4 ± 9.9 years). None of the patients had other coexistent conditions that might affect the brain WM. To obtain normative data, we included 61 individuals in the same age range who underwent MRI for other reasons (mild developmental delay, autism, epilepsy, tics, headache) and had a normal MRI and neurologic examination. Thirty-three were male, 28 female; age range was 0.3 to 44 years (mean age ± SD: 7.9 ± 9.4 years). Some control participants underwent only part of the quantitative MRI protocol (table e-1 on the *Neurology*® Web site at Neurology.org).

MR acquisition. All studies were conducted on the same MR machine at 1.5T (Siemens Sonata, Erlangen, Germany) with an 8-channel phased-array head coil. The conventional imaging protocol included axial T2-weighted spin echo images, axial fluid-attenuated inversion recovery images, and sagittal T1-weighted images using a 3-dimensional magnetization-prepared rapid-acquisition gradient echo sequence.

For MR spectroscopy with chemical shift imaging (CSI), we used PRESS (point-resolved spectroscopy) (repetition time [TR]/echo time [TE] 3,000/30 milliseconds [ms], 6 acquisitions with weighted phase encoding) on a single 15-mm slice (field of view 120–160 × 160 mm^2 depending on head size, volume of interest 60–80 × 100 mm^2, 16 × 16 phase encodings, voxel size 7.5–10 × 10 × 15 mm^3) centered onto the corpus callosum. Unsuppressed water reference scans were obtained with head and body coil.[17]

For diffusion tensor imaging (DTI), we used a multislice echo planar imaging sequence (TR/TE 6,700/81 ms, b value 750 s/mm^2, 12 directions, 2 acquisitions, 1 b0 volume, 49 slices, pixel size 2.5 × 2.5 × 2.5 mm^3, no parallel imaging). One of the slices corresponded to the center of the CSI slice.

For T2 relaxometry, we used a Carr-Purcell-Meiboom-Gill sequence to acquire images at 32 different echo times (TR 2,500 ms, TE 10.4–332.8 ms, spacing 10.4 ms, 5 slices, pixel

Table 1 Overview of the patients with hypomyelination

Patient	Age at MRI, y	Sex	Cause	Method of diagnosis	GMFCS
1	10.3	M	4H	DNA-based	2
2	17.6	F	4H	DNA-based	2
3	19.3	F	4H	DNA-based	5
4	1.5	M	HABC	DNA-based	5
5	2.8	F	HABC	DNA-based	3
6	5.9	F	HABC	DNA-based	4
7	10.6	M	HCC	DNA-based	4
8	13.3	M	HCC	DNA-based	4
9	47.2	F	ODDD	DNA-based	2
10	0.8	M	PMD	DNA-based	5
11	1.8	M	PMD	DNA-based	5
12	1.9	M	PMD	DNA-based	2
13	7.0	M	PMD	DNA-based	3
14	20.9	M	PMD	DNA-based	5
15	11.0	M	PMLD	DNA-based	4
16	0.5	F	RARS	DNA-based	4
17	2.4	F	RARS	DNA-based	3
18	16.8	M	RARS	DNA-based	4
19	4.1	F	Salla	DNA-based	4
20	4	F	Unknown		5
21	5.4	F	Unknown		1
22	5.4	F	Unknown		1
23	7.3	F	Unknown		1
24	12.6	M	Unknown		2
25	14.7	M	Unknown		2
26	15.6	F	Unknown		1
27	27.4	F	Unknown		5
28	30.5	F	Unknown		1

Abbreviations: 4H = hypomyelination with hypogonadotropic hypogonadism and hypodontia; GMFCS = gross motor function classification system; HABC = hypomyelination with atrophy of the basal ganglia and cerebellum; HCC = hypomyelination with congenital cataract; ODDD = oculodentodigital dysplasia; PMD = Pelizaeus-Merzbacher disease; PMLD = PMD-like disease; RARS = hypomyelination with *RARS* mutations.

size 1 × 1 × 5 mm^3). The middle slice corresponded to the center of the CSI slice.

For magnetization transfer imaging, we used a 3-dimensional FLASH (fast low-angle shot) sequence obtaining 2 sets of images: one with a magnetization transfer saturation pulse (7.68-ms gaussian radiofrequency pulse 1,500 Hz off-resonance [M_s]) and one without (M_0). Imaging measures included TR/TE 23/4.7 ms, pixel size 1 × 1 × 4 mm^3, and 32 slices, with one of the slices corresponding to the center of the CSI slice.

Data processing and analysis. We quantified metabolite concentrations measured by CSI as described before using LCModel[18]; metabolite concentrations were reported in millimole/liter. For generation of pixel-wise T2 maps, we fitted the relaxation time curves to a mono-exponential decay: $S(t) = S(0)\exp(-t/T2)$. We created magnetization transfer ratio (MTR) maps according to the equation $MTR = 1 - (M_s/M_0)$. We used the FMRIB Software Library (http://www.fmrib.ox.ac.uk/fsl) to analyze DTI data, resulting in maps of fractional anisotropy (FA), AD, RD, and mean diffusivity (MD) (or apparent diffusion coefficient). FA images from multiple participants were aligned into a common space with tract-based spatial statistics (TBSS) and a mean FA skeleton was created. Each participant's aligned FA data were projected onto this skeleton and fed into voxel-wise cross-participant statistics using Randomize, with age as covariate.[19]

We estimated DTI measures and T2 and MTR values in 3 WM regions of interest (ROIs), representing different phases during normal myelination: early myelination (corticospinal tracts in the centrum semiovale), intermediate myelination (splenium), and late myelination (parietal deep WM). The advantage of including the splenium is that it does not contain fibers with different orientations ("crossing fibers"). DTI ROIs, positioned in standard space, were identical for all participants. We manually placed ROIs on T2 and MTR maps based on visual matching with DTI ROIs. In some patients, the splenium was very thin, hampering ROI positioning (table e-1). Regarding CSI, we included voxels in the analyses that best corresponded to the parietal deep WM ROIs, as well as voxels containing the corticospinal tracts. The splenium of the corpus callosum was not present in the CSI slab and therefore not included. Values of left and right hemispheres were averaged. Using TBSS, we further evaluated DTI measures by estimating the percentage of the WM skeleton that was significantly different from controls (threshold-free cluster enhancement [TFCE]-corrected $p < 0.01$). For the voxels, in which all DTI metrics were significantly different between patient and control values, we extracted the DTI values and averaged them for patients and controls.

Motor handicap. Because there is no standardized tool to assess motor performance in hypomyelinating disorders, we used the quantitative, validated, and widely used gross motor function classification system (GMFCS)[20] to score the severity of motor handicap at the time of MRI to allow comparison of motor function with quantitative MR measures. Two experienced investigators (M.E.S., N.I.W.) separately assessed patients based on medical files.

To evaluate the correlation between GMFCS and quantitative MR measures, we used the parietal deep WM ROI and the ROI containing the corticospinal tracts in the centrum semiovale.

Statistical analysis. We constructed 3 datasets, one comprising patient values, a second containing control values, and a third with calculated control values age-matched per patient, based on a mono-exponential fit through the control measures: a + b exp(−age/tau). Parameters a (limiting value), b (difference between limiting value and value at age 0 years), and tau (time constant) were estimated using nonlinear least squares (table e-2).

To assess whether the MR measures were significantly different between patients and controls, we first removed the dependency on age by subtraction of an isotonic regression curve fitted jointly (as appropriate under the null hypothesis) on both groups. Subsequently, we used the Wilcoxon rank sum test to compare the resulting age-corrected characteristics (residuals) of the 2 groups.

To evaluate a possible distinction between AD and RD, we transformed the data of patients and controls to rank data followed by fitting of an isotonic regression curve between the rank data and age and obtaining the residual ranks from this analysis. We used the Wilcoxon test to assess the significance of differences between AD and RD.

We used linear regression analyses to correlate GMFCS and quantitative MR measures. Missing MR measure data of patients

Table 2 Quantitative magnetic resonance measures in patients with hypomyelination and controls obtained with region of interest analyses

	Splenium				Corticospinal tracts				Parietal deep WM			
	Patients[a]	Controls[a]	Difference[b]	Relative difference, %	Patients[a]	Controls[a]	Difference[b]	Relative difference, %	Patients[a]	Controls[a]	Difference[b]	Relative difference, %
FA	0.45[c] (0.14)	0.74 (0.10)	−0.32 (0.2)	−41 (19)	0.28[c] (0.06)	0.35 (0.06)	−0.09 (0.06)	−25 (17)	0.21[c] (0.04)	0.28 (0.04)	−0.09 (0.04)	−30 (14)
MD, 10^{-5} mm²/s	142[c] (45)	93 (21)	54 (47)	65 (57)	95[c] (12)	84 (9)	16 (11)	20 (14)	109[c] (12)	95 (8)	19 (13)	21 (14)
AD, 10^{-5} mm²/s	216[c] (46)	191 (22)	30 (47)	16 (26)	123[c] (13)	116 (9)	10 (13)	9 (11)	132[c] (12)	123 (8)	13 (12)	11 (10)
RD, 10^{-5} mm²/s	105[c] (47)	45 (23)	67 (49)	191 (148)	81[c] (13)	67 (9)	19 (12)	30 (19)	98[c] (13)	81 (9)	21 (13)	28 (18)
T2, ms	182[c] (41)	101 (29)	85 (33)	89 (37)	149[c] (25)	107 (9)	44 (23)	42 (22)	152[c] (24)	108 (15)	48 (21)	46 (21)
MTR	0.20[c] (0.05)	0.34 (0.04)	−0.14 (0.05)	−41 (14)	0.22[c] (0.06)	0.34 (0.02)	−0.12 (0.06)	−36 (19)	0.20[c] (0.06)	0.32 (0.03)	−0.12 (0.05)	−38 (16)
Cr, mM					5,1[c] (1.1)	4.4 (0.7)	0.8 (1.2)	20 (28)	4.7[c] (1.0)	4.0 (0.5)	0.7 (1.0)	19 (26)
NAA, mM					6.6[c] (2.3)	7.2 (1.0)	−0.8 (2.0)	−12 (27)	6.3[c] (1.9)	6.9 (0.9)	−0.8 (1.8)	−12 (25)
Cho, mM					1.32[c] (0.31)	1.55 (0.23)	−0.18 (0.29)	−12 (20)	1.15[c] (0.32)	1.53 (0.22)	−0.32 (0.29)	−22 (20)
Ins, mM					4.7[c] (1.1)	3.0 (0.5)	2.0 (1.2)	69 (41)	5.0[c] (1.5)	3.3 (0.5)	1.7 (1.5)	53 (46)
NAA/Cr					1.28[c] (0.28)	1.67 (0.29)	−0.49 (0.29)	−27 (15)	1.34[c] (0.29)	1.73 (0.26)	−0.48 (0.27)	−26 (15)

Abbreviations: AD = axial diffusivity; Cho = choline; Cr = creatine; FA = fractional anisotropy; Ins = myo-inositol; MD = mean diffusivity; MTR = magnetization transfer ratio; NAA = *N*-acetylaspartate; RD = radial diffusivity; WM = white matter.
Data represent mean (SD).
[a] Mean values of patients and controls are arithmetic averages of values, irrespective of age.
[b] Difference between patients and controls is based on the actual patient values compared to the mono-exponential fit of the control values as a function of age (as described in the methods section).
[c] Statistically significant difference between patients and controls (Wilcoxon rank sum test).

were imputed using a nonparametric k-nearest neighbor method.[21] First analysis comprised simple linear regression linking handicap to individual measures. Subsequently, we built a multiple linear regression model with a preference of the more parsimonious model. Model search was performed in a backward manner, first including all explanatory variables and then removing them one by one. We used selection frequency, based on application of lasso regression to 1,000 resampled versions of the dataset, as an inclusion criterion; cross-validation determined the lasso penalty measure. We chose the final model to minimize the number of explanatory variables without compromising the coefficient of determination.

RESULTS Table e-1 presents the number of included MR studies per quantitative method. Figure 1 shows examples of the FA, RD, MTR map, T2 map, and CSI spectrum. Figure e-1 shows diagrams of MR measures vs age per WM area.

DTI, T2 relaxometry, and magnetization transfer imaging. In the ROI analysis, FA was lower in patients than in controls in all areas. Regional distribution was similar in patients and controls: FA of the splenium was higher than that of the other WM areas. The decrease in FA in patients relative to age-matched controls was also largest in the splenium. AD, RD, and MD were higher in patients than in controls. Patients had the highest values of AD, RD, and MD in the splenium, and differences for these measures compared with controls were also largest in the splenium (figure e-1, table 2). When AD and RD were compared, the increase in RD was significantly greater relative to age-matched control values than the increase in AD (Wilcoxon rank sum test: $p = 0.008$ for splenium; $p = 0.027$ for corticospinal tracts in the centrum semiovale; $p = 0.002$ for deep parietal WM). In all WM areas, MTR values were lower in patients than in controls (figure e-1, table 2), while T2 values were higher.

For the TBSS analysis, we created a mean WM skeleton, shown in green in figure 2. When we compared DTI measures of patients with those of controls within the skeleton, extensive changes in all DTI measures were observed. FA was lower in patients than in controls in as much as 96% of the whole skeleton (TFCE-corrected threshold <0.01). RD was increased in 93% of the skeleton, and MD in 84% of the skeleton. AD was increased in only 20% of the skeleton. These latter areas were confined to the splenium, small part of the genu, corona radiata, parts of the superior longitudinal fasciculus, and parts of the thalamic radiation (figure 2, D–F). Table 3 shows mean values of the measures within the area that was significantly abnormal for all DTI metrics (20% of the skeleton; TFCE-corrected threshold <0.01). Although all voxels within this area had significantly increased AD, the relative increase in AD of 13% was much smaller than the 35% increase

Figure 2 TBSS images

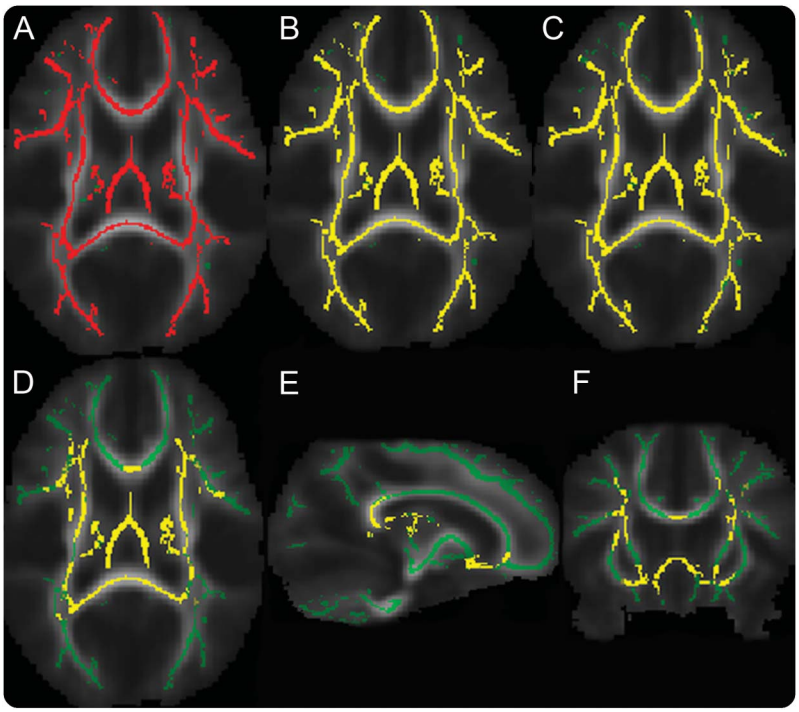

TBSS images depicting (A) decreased fractional anisotropy (red), (B) increased radial diffusivity (yellow), (C) increased mean diffusivity (yellow), and (D–F) increased axial diffusivity (yellow) at threshold-free cluster enhancement–corrected $p < 0.01$ in patients with hypomyelination vs controls overlaid on skeleton (green). TBSS = tract-based spatial statistics.

in RD, in agreement with the significantly larger increase of RD than AD in the ROI analysis.

Chemical shift imaging. CSI results were similar for the parietal deep WM and corticospinal tracts in the centrum semiovale. Choline (Cho)-containing compounds were lower and myo-inositol (Ins) was higher in patients than in controls. *N*-acetylaspartate, including *N*-acetylaspartylglutamate (NAA), and creatine (Cr) and phosphocreatine (Cr) mainly showed decreases and increases, respectively (figure e-1, table 2). To correct for possible effects of higher axonal density per tissue volume caused by lower density of myelin sheaths on NAA values, we also evaluated the ratio NAA/Cr. NAA/Cr values were either normal or reduced in patients compared with controls (figure e-1).

Table 3 DTI measures in patients with hypomyelination and controls within the part of the white matter skeleton that is abnormal for all DTI metrics (20% of the skeleton)

MR measure	Patients	Controls	Absolute difference	Relative difference, %
FA	0.31 (0.05)	0.40 (0.05)	−0.09	−24
MD, 10^{-5} mm²/s	115 (15)	93 (11)	23	24
AD, 10^{-5} mm²/s	154 (15)	135 (9)	18	13
RD, 10^{-5} mm²/s	97 (16)	72 (12)	25	35

Abbreviations: AD = axial diffusivity; DTI = diffusion tensor imaging; FA = fractional anisotropy; MD = mean diffusivity; MR = magnetic resonance; RD = radial diffusivity.
Data represent mean (SD) or mean. MR measures were significantly different between patients and controls at a threshold-free cluster enhancement–corrected threshold <0.01.

Motor handicap correlated with quantitative MR measures. The motor handicap of the patients assessed by the GMFCS is summarized in table 1. Regression analyses of quantitative MR measures in the parietal deep WM revealed MTR and RD as measures with the largest coefficients of determination individually (0.48 and 0.46, respectively); NAA/Cr (R_2 0.37) and T2 (R_2 0.35) had reasonable coefficients of determination as well. The other measures did not correlate well with motor handicap (R_2: NAA 0.17, AD 0.13, Ins 0.07, Cho 0.008, Cr 0). Multiple linear regression analyses indicated that the most parsimonious model included NAA/Cr and RD. MTR and T2 could be added to the model but did not lead to improvement of the coefficient of determination. Ins, Cho, and AD did not add anything to the model. The final model was given by GMFCS $= 0.33 + 6 \times 10^3 \times \text{RD} - 2.29 \times \text{NAA/Cr}$ with p values <0.001 for RD and <0.01 for NAA/Cr (Student t test). The model explained 58% of the variance in GMFCS.

Analysis with the results of the quantitative MR measures in the ROI containing the corticospinal tracts yielded a final model that expressed GMFCS in terms of RD and NAA/Cr as well, with 51% of variance explained.

DISCUSSION Our aim was to gain insight into tissue measures that account for unexplained variability in motor handicap among patients with hypomyelination, which could serve to monitor future therapies. The changes we found in quantitative MR measures in the WM are in line with lack of myelin, with low FA, high RD and AD, high T2 relaxation times, low MTR, and low Cho, and to a lesser degree with compromised axonal integrity with slightly elevated AD and decreased NAA/Cr. The variation in GMFCS was in part (58%) explained by the measures obtained in the parietal deep WM; the results for the area containing the corticospinal tracts were similar. Individually, RD, NAA/Cr, MTR, and T2 all correlated with GMFCS; NAA/Cr and RD were the strongest independent predictors.

Measurements of AD and RD in hypomyelination have not been reported previously. RD has been suggested to correlate with amounts and integrity of myelin[15,16] and AD with axonal integrity.[13,14] Because the interpretation of AD and RD in crossing fiber regions requires caution,[22] we also included the splenium. RD had the strongest correlation with GMFCS; AD showed a much weaker correlation. The increase in RD was larger and much more widespread than the change in AD (93% vs 20% of the skeleton), with a normal AD in large areas in which

conventional images indicate lack of myelin. DTI measures in the splenium were distinct from DTI measures in the other WM regions in that the differences between patients and controls were larger. Partial volume effects with inclusion of CSF in the ROIs may explain these findings, as in many patients the splenium had reduced thickness. Partial volume correction by the method of free water elimination might reduce this problem in future studies.[23,24]

MTR has been interpreted as a measure representing myelin integrity, although it has also been correlated with axonal integrity.[25] In our study, MTR alone correlated strongly with GMFCS, but was not selected as an independent explanatory variable. MTR is correlated with RD and NAA/Cr, and in the regression analysis, the combination of these latter 2 variables yielded the most parsimonious model without a significant extra contribution of MTR.

NAA was low to normal in the WM of patients. NAA, although synthesized and degraded in glia, is mainly located in neurons and axons and is a useful surrogate marker for axonal integrity and density.[26,27] The relatively normal NAA in some patients could be interpreted as evidence of relative axonal integrity, but the explanation is more complex. High WM concentrations of NAA have been reported before in hypomyelination,[28] probably reflecting higher axonal density in the absence of normal myelin density. Dividing NAA by Cr, reflecting cell density in general, corrects at least partially for higher compaction due to lack of myelin. Whereas NAA and Cr individually did not correlate with the GMFCS, NAA/Cr did, suggesting that axonal damage does contribute to the motor handicap in hypomyelinating disorders, although to a lesser degree than lack of myelin considering the relatively small change in AD.

The above results are in line with existing evidence that RD is correlated inversely with amount and integrity of myelin and indicate that myelin is a stronger determiner of handicap in patients with hypomyelination than axonal integrity.

All odds were against this study with a rather small number of patients, heterogeneous diagnoses each associated with private effects on handicap and MR measures, large patient age variation, acquisition of quantitative MR measures in only 3 brain areas, and the neurologic health of controls not being fully guaranteed. Hypomyelinating disorders are very rare diseases with many different known and often unknown causes.[10,29] A group of 28 patients investigated on one MR system is actually large. Ideally, only healthy participants would be included as controls, but this is not an option for very young children who need anesthesia or sedation. Despite normal neurologic examination and MRI, the controls had some complaints and their quantitative measures were probably more variable than in completely healthy participants.

The fact that we did find a correlation between quantitative MR measures and the severity of motor handicap despite these odds corroborates the results. Because we found this correlation in a group of hypomyelinating disorders with different causes and underlying pathologies, it is likely that the correlation would be even stronger in studies on single hypomyelinating disorders. That we found this correlation while comparing patients with control subjects with some neurologic complaints indicates that the correlation may actually be stronger. The correlation between quantitative brain MR measures and clinical handicap was found, while only 3 brain areas were investigated. If more areas, especially brainstem and spinal cord tracts would be included, the correlation would increase. Future longitudinal studies including more extensive serial MRI measurements and clinical follow-up should give the opportunity to further support the results of the present cross-sectional study.

Hypomyelinating disorders constitute a large fraction of the leukodystrophies, for which therapies are urgently needed. The fact that measures representing myelin integrity (RD) show a stronger correlation with motor handicap than measures of axonal integrity (NAA/Cr, AD) is a highly promising finding in view of strategies aimed at promotion of myelination. Objective measures to evaluate the success of novel therapies, such as neural stem cell engraftment,[30] are necessary. Our study indicates that quantitative MR can be useful to monitor outcome.

AUTHOR CONTRIBUTIONS

M.E. Steenweg, N.I. Wolf, W.N. van Wieringen, and F. Barkhof contributed to the conception of the study, analysis and interpretation of the data, and editing of the manuscript. M.S. van der Knaap and P.J.W. Pouwels are the principal investigators. They designed the study, contributed to the analysis and interpretation of the data, and revised the manuscript.

ACKNOWLEDGMENT

The authors thank all the patients, families, and colleagues who contributed to the studies.

STUDY FUNDING

The study received financial support from the Dutch Organization for Scientific Research (ZonMw, TOP Grant 9120.6002) and the Optimix Foundation for Scientific Research.

DISCLOSURE

M. Steenweg, N. Wolf, and W. van Wieringen report no disclosures relevant to the manuscript. F. Barkhof serves as a consultant for Bayer Schering Pharma, Sanofi-Aventis, Biogen Idec, Teva, Novartis, Roche, Synthon BV, and Jansen Research. M. van der Knaap and P. Pouwels report no disclosures relevant to the manuscript. Go to Neurology.org for full disclosures.

Received November 11, 2015. Accepted in final form March 12, 2016.

REFERENCES

1. Brockmann K, Finsterbusch J, Terwey B, Frahm J, Hanefeld F. Megalencephalic leukoencephalopathy with subcortical cysts in an adult: quantitative proton MR spectroscopy and diffusion tensor MRI. Neuroradiology 2003; 45:137–142.

2. Dreha-Kulaczewski SF, Brockmann K, Henneke M, et al. Assessment of myelination in hypomyelinating disorders by quantitative MRI. J Magn Reson Imaging 2012;36:1329–1338.
3. Steenweg ME, Pouwels PJ, Wolf NI, van Wieringen WN, Barkhof F, van der Knaap MS. Leukoencephalopathy with brainstem and spinal cord involvement and high lactate: quantitative magnetic resonance imaging. Brain 2011;134:3333–3341.
4. Vermathen P, Robert-Tissot L, Pietz J, Lutz T, Boesch C, Kreis R. Characterization of white matter alterations in phenylketonuria by magnetic resonance relaxometry and diffusion tensor imaging. Magn Reson Med 2007;58:1145–1156.
5. van der Voorn JP, Pouwels PJ, Salomons GS, Barkhof F, van der Knaap MS. Unravelling pathology in juvenile Alexander disease: serial quantitative MRI and spectroscopy of white matter. Neuroradiology 2009;51:669–675.
6. van der Voorn JP, Pouwels PJ, Hart AA, et al. Childhood white matter disorders: quantitative MR imaging and spectroscopy. Radiology 2006;241:510–517.
7. van der Voorn JP, Pouwels PJ, Powers JM, et al. Correlating quantitative MR imaging with histopathology in X-linked adrenoleukodystrophy. Am J Neuroradiol 2011;32:481–489.
8. Bizzi A, Castellis G, Bugiani M, et al. Classification of childhood white matter disorders using proton MR spectroscopic imaging. Am J Neuroradiol 2008;29:1270–1275.
9. Barker PB, Horská A. Neuroimaging in leukodystrophies. J Child Neurol 2004;19:559–570.
10. Schiffmann R, van der Knaap MS. Invited article: an MRI-based approach to the diagnosis of white matter disorders. Neurology 2009;72:750–759.
11. Wolf NI, Vanderver A, van Spaendonk RML, et al. Clinical spectrum of 4H leukodystrophy caused by POLR3A and POLR3B mutations. Neuology 2014;83:1898–1905.
12. Pouwels PJ, Vanderver A, Bernard G, et al. Hypomyelinating leukodystrophies: translational research progress and prospects. Ann Neurol 2014;76:5–19.
13. Budde MD, Xie M, Cross AH, Song SK. Axial diffusivity is the primary correlate of axonal injury in the experimental autoimmune encephalomyelitis spinal cord: a quantitative pixelwise analysis. J Neurosci 2009;29:2805–2813.
14. Sun SW, Liang HF, Cross AH, Song SK. Evolving Wallerian degeneration after transient retinal ischemia in mice characterized by diffusion tensor imaging. Neuroimage 2008;40:1–10.
15. Song SK, Sun SW, Ramsbottom MJ, Chang C, Russell J, Cross AH. Dysmyelination revealed through MRI as increased radial (but unchanged axial) diffusion of water. Neuroimage 2002;17:1429–1436.
16. Song SK, Yoshino J, Le TQ, et al. Demyelination increases radial diffusivity in corpus callosum of mouse brain. Neuroimage 2005;26:132–140.
17. Pouwels PJW, Steenweg ME, Barkhof F, van der Knaap MS. Absolute metabolite quantification in human brain using short echo-time CSI and a phased-array head-coil. Proceedings of the Annual Meeting of ISMRM; May 1–7, 2010; Stockholm; 3336.
18. Provencher SW. Estimation of metabolite concentrations from localized in vivo proton MR spectra. Magn Reson Med 1993;30:672–679.
19. Smith SM, Jenkinson M, Johansen-Berg H, et al. Tract-based spatial statistics: voxelwise analysis of multi-subject diffusion data. Neuroimage 2006;31:1487–1505.
20. Palisano R, Rosenbaum P, Walter S, Russell D, Wood E, Galuppi B. Development and reliability of a system to classify gross motor function in children with cerebral palsy. Dev Med Child Neurol 1997;39:214–223.
21. Troyanskaya O, Cantor M, Sherlock G, et al. Missing value estimation methods for DNA microarrays. Bioinformatics 2001;17:520–525.
22. Wheeler-Kingshott CA, Cercignani M. About "axial" and "radial" diffusivities. Magn Reson Med 2009;61:1255–1260.
23. Metzler-Baddeley C, O'Sullivan MJ, Bells S, Pasternak O, Jones DK. How and how not to correct for CSF-contamination in diffusion MRI. Neuroimage 2012;59:1394–1403.
24. Pasternak O, Sochen N, Gur Y, Intrator N, Assaf Y. Free water elimination and mapping from diffusion MRI. Magn Reson Med 2009;62:717–730.
25. van Waesberghe JH, Kamphorst W, De Groot CJ, et al. Axonal loss in multiple sclerosis lesions: magnetic resonance imaging insights into substrates of disability. Ann Neurol 1999;46:747–754.
26. Bjartmar C, Battistuta J, Terada N, Dupree E, Trapp BD. N-acetylaspartate is an axon-specific marker of mature white matter in vivo: a biochemical and immunohistochemical study on the rat optic nerve. Ann Neurol 2002;51:51–58.
27. Brooks WM, Sibbitt WL Jr, Kornfeld M, Jung RE, Bankhurst AD, Roldan CA. The histopathologic associates of neurometabolite abnormalities in fatal neuropsychiatric systemic lupus erythematosus. Arthritis Rheum 2010;62:2055–2063.
28. Hanefeld FA, Brockmann K, Pouwels PJ, Wilken B, Frahm J, Dechent P. Quantitative proton MRS of Pelizaeus-Merzbacher disease: evidence of dys- and hypomyelination. Neurology 2005;65:701–706.
29. van der Knaap MS, Breiter SN, Naidu S, Hart AA, Valk J. Defining and categorizing leukoencephalopathies of unknown origin: MR imaging approach. Radiology 1999;213:121–133.
30. Gupta N, Henry RG, Strober J, et al. Neural stem cell engraftment and myelination in the brain. Sci Transl Med 2012;4:155ra137.